Biochimica et Biophysica Acta, 1152 (1993) 207–218

BBAMEM 76121

Electrical properties of cell pellets and cell electrofusion in a centrifuge

I.G. Abidor [a], A.I. Barbul [a], D.V. Zhelev [c], P. Doinov [c], I.N. Bandrina [b], E.M. Osipova [a] and S.I. Sukharev [a,*]

[a] *A.N. Frumkin Institute of Electrochemistry, Russian Academy of Sciences, Moscow (Russia),* [b] *V.A. Engelhardt Institute of Molecular Biology, Russian Academy of Sciences, Moscow (Russia) and* [c] *Central Biophysical Laboratory of Bulgarian Academy of Sciences, Sofia (Bulgaria)*

(Received 27 April 1993)
(Revised manuscript received 21 July 1993)

Key words: Cell electrofusion; Membrane electroporation; Intercellular contact; Cell deformation; Membrane fusion

A new approach is proposed for studying cell deformability by centrifugal force, electrical properties of cell membranes in a high electric field, and for performing efficient cell electrofusion. Suspensions of cells (L929 and four other cell types examined) are centrifuged in special chambers, thus forming compact cell pellets in the gap between the electrodes. The setup allows measurement of the pellet resistance and also the high-voltage pulse application during centrifugation. The pellet resistance increases sharply with the centripetal acceleration, which correlates with reduction of the cell pellet porosity due to cell compression and deformation. Experiments with cells pretreated with cytochalasin B or colcemid showed that cell deformability depends significantly on the state of cytoskeleton. When the voltage applied to the cell pellet exceeds a 'critical' value, electrical breakdown (poration) of cell membranes occurs. This is seen as a deflection in the $I(V)$ curve for the cell pellet. The electropores formed during the breakdown reseal in several stages: the fastest takes 0.5–1 ms while the whole process completes in minutes. A novel effect of colloid-osmotic compression of cell pellets after electric cell permeabilization is described. Supercritical pulse application to the cell pellet during intensive centrifugation leads to massive cell fusion. The fusion index grows with the increase of centripetal acceleration, and drops drastically when the pulse is applied after the centrifuge is stopped. The colloid-osmotic pellet compression enhances the fusion efficiency. No fusion occurs when cells are brought in contact after the pulse treatment. The data suggest that tight intermembrane contact formed prior to pulse application is a prerequisite condition for efficient cell electrofusion. The capacities of the technique proposed and the mechanism of membrane electrofusion are discussed.

Introduction

A basic effect observed on any cell type or model membrane system, subjected to high electric fields, is an electric breakdown of membranes, i.e., sharp increase in non-specific membrane conductance and permeability, due to aqueous pore formation (electroporation). This phenomenon has been investigated extensively, primarily by two approaches: (i), using direct electrical measurements (voltage clamp or charge-pulse relaxation techniques) on single cells and planar bilayers to study initial events in membrane pore formation and also pore development [1–6] and (ii), permeability tests on cell or lipid vesicle suspensions using probe molecules of different sizes after application of external electric fields that enabled one to estimate the mean size and lifetime of electropores [7–9].

In 1979 Kinosita and Tsong reported a direct recording of breakdown currents through dense suspensions of human erythrocytes [10]. The authors resolved the kinetics of pore formation and pore resealing, and estimated the number of conducting pores per cell. Teissie and Tsong [11] identified the nature of some of those pores using the same approach. The advantage of using dense cell suspensions was an automatic averaging of 'microscopic' currents through each cell over all cells in the population. An alternative to cell suspension is use of compact cell pellets to minimize the electric current through the extracellular medium and to increase the resolution of current measurements.

The electric properties of compressed cell pellets may be helpful in describing the phenomenon of cell

* Corresponding author. Present address: University of Wisconsin, Laboratory of Molecular Biology, 1525 Linden Drive, Madison, WI 53706, USA. Fax: +1 (608) 2624570.

fusion induced by pulsed electric field (electrofusion). Discovered by Senda in 1979 [12], cell electrofusion is now regarded as an advanced method in cell and developmental biology [13–15]. Electrofusion procedure is usually performed in three steps: (i), the creation of tight intercellular contact (by means of dielectrophoresis [13,14], agglutination [16], confluent monolayer [17] or double cell layer formation [18], etc.); (ii), high-voltage pulse application, which induces membrane fusion and (iii), incubation of cell pairs in appropriate conditions allowing the fusion of the cytoplasm. Does cell fusion occur directly in an electric field or do the electric pulses transform the membrane structure to a long-lived fusogenic state [19,20] during which the membranes fuse spontaneously?

In the present work we provide a detailed description of a new efficient technique for cell electrofusion in a centrifuge [21,22]. A compact cell pellet formed under controlled centrifugation and subjected to a high electric field gives insights into some of the relationships between membrane contact, electric pore formation and cell fusion. We have also discovered a significant effect of colloid-osmotic cell swelling on the geometry of intercellular contacts in pellets.

Materials and Methods

Cells

L-929, NIH3T3, HeLa, CHO and E2 cell (rat embryo fibroblasts immortalized with E1A oncogene) were received from the Cell Culture Collection of the Institute of Cytology of the Russian Academy of Sciences (St. Petersburg, Russia). All the cell lines were grown in DMEM (Gibco) supplemented with 10% newborn calf serum (NBS, Gibco) and 40 μg/ml gentamycin for 48 h. After standard trypsinization procedure, cells were washed twice with PBS (PM16, Serva, Ca^{2+} and Mg^{2+} free) and then suspended in pulsation buffer, PBS with isotonic (290 mM) sucrose solution in 2:1 (v/v) ratio. In some experiments cells were pretreated with cytochalasin B (Calbiochem) or colcemid (Sigma). Cytochalasin B (2 μg/ml) or colcemid (0.5–1 μg/ml) in DMEM were added to culture flasks 3 or 10 h prior to experiment, respectively. Each of these substances was present in the pulsation buffer at the given concentration.

Centrifuge and electronic setup

A desk-top centrifuge (Type 310, Mechanica Precyzyjna, Poland) equipped with a laboratory-built rotor carrying a pair of special chambers was used for pelleting cells (see Fig. 1). Each chamber consisted of a teflon socket (1.5 ml) with a 1 or 3-mm diameter hole at the bottom. The bottom and top stainless steel electrodes were fixed by screws, and the gap between them was adjusted to 2 mm. During centrifugation, the cells were collected from a suspension into the hole and formed a compact pellet on the bottom electrode. A stable electric connection between the chambers and the electronic setup during centrifugation was provided by contact disks on the rotor head, and a pair of brushes mounted on the centrifuge lid. Typically, only one chamber was used for the electric measurements, while the second chamber, electrically isolated, was used as a counter-balance.

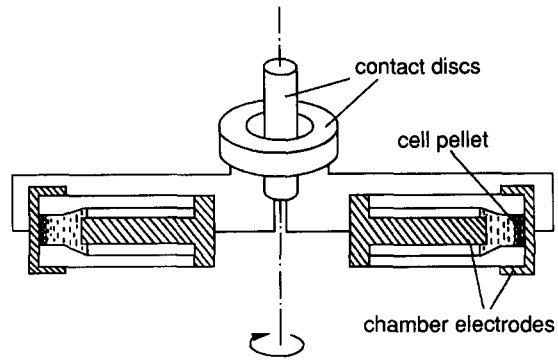

Fig. 1. The chamber and rotor design. The rotor carries two chambers consisting of a teflon socket and stainless steel electrodes (shaded). The later are connected to the electronic setup by a pair of brushes (not shown) slipping on two contact discs. Cell pellets are formed on the bottom electrodes. Usually, only one chamber was used for electric measurements, while the second one, electrically isolated, was used as a counterbalance.

The setup used for most of the experiments (Fig. 2a) was a combination of two circuits commutated by a high-voltage switch. The high-voltage circuit allowed the application of square voltage pulses (0–1 kV amplitude, 15–100 μs duration) to the cell pellet and the measurement the chamber current during the pulse. By means of the low-voltage circuit, we measured the chamber current in response to the 0.1–1-V, 10-kHz sine-wave test signal. The centrifuge rotation speed was controlled by a stroboscopic tachometer.

Cell pellet compression measurement

The low-voltage pellet resistance (R_p) was taken as an inverse measure of the pellet porosity. At a given number of cells and pellet geometry, the increase in R_p reflected tightening of cell package, and consequently decrease in pellet porosity. The chamber current changes upon pellet compression by centrifugal force were registered in the presence of a 0.1–2 V, 10 kHz AC test signal using a current-to-voltage converter (Keithley 427), AC-voltmeter (V3-57) and chart recorder (REC1, Pharmacia, Sweden) (Fig. 2a). The test signal was delivered from the G_1 generator (PSI, model A100, UK).

Electrical membrane poration

The extent of membrane poration was determined by the current through the pellet. The current was

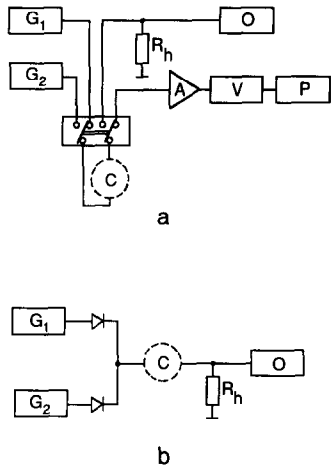

Fig. 2. Experimental setups. (a) The setup designed for cell electrofusion and for measurements of chamber currents at low-voltage and high-voltage stimuli. It consists of two circuits, connected to the chamber (C) via high-voltage switch. Low-voltage AC signals (0.1–3 V, 10 kHz) are applied from the sine-wave generator (G_1). The chamber current is measured by current-to-voltage converter (A), rectifying voltmeter (V) and chart recorder (P). High-voltage pulses (0–1 kV, 15–100 μs) are delivered from the G_2 generator and the going-through currents are recorded using the load resistor R_h (1 or 10 Ω) and the storage oscilloscope (O). (b) The setup for electrical recording of membrane resealing process. Single high-voltage pulses applied from the generator (G_2) are followed by a train of test pulses (10 V, 10 μs) from pulse generator G_1. The current is recorded by the load resistor ($R_h = 10\ \Omega$) and storage oscilloscope (O).

measured during high-voltage pulses delivered from the high-voltage laboratory-built generator using the load resistor ($R_h = 1$ or 10 Ω) and storage oscilloscope (S8-13). The values of the current recorded at the end of each 30-μs pulse were plotted vs. pulse amplitude. The instantaneous current-to-voltage relations for different cell pellets were evaluated.

Membrane resealing

The membrane resealing process was recorded electrically using the circuit shown in Fig. 2b. The cell pellets were subjected to a single high-voltage pulse (from a G_2 generator) followed by a series of test pulses (10 V, 10 μs, 50 μs period), delivered from the G_1 generator (Hewlett-Packard 214B). The envelopes of current responses upon test pulses reflected the kinetics of cell pellet conductivity after electric breakdown. The low-voltage test pulses did not affect the conductance of the cell pellet (not shown).

Cell electrofusion in the centrifuge

Typically, 0.5-ml aliquots of suspension containing $2 \cdot 10^6$ cells were placed into the chamber (with 3 mm hole) and centrifuged at 400–600 $\times g$ for 10 min (prepulse centrifugation). One or two pulses of 300–800 V (i.e., 1.5–4 kV/cm) amplitude and 20–50 μs duration were than applied during rotor spinning at a given acceleration G. After 5 min of post-pulse centrifugation the chamber was incubated for 20 min at 37°C, then 1 ml of DMEM, supplemented with 15% NBS was added. Cells were suspended gently and seeded on coverslips in a 12-well culture plate (Costar). After incubation for 16–24 h at 37°C in an atmosphere with 5% CO_2, the preparations of plated cells were fixed with 70% ethanol and stained with the Giemsa solution (Merck). Fused cells were counted microscopically and the fusion (polynucleation) index F was expressed as

$$F = (N_p / N) \cdot 100\% - F_o \quad (1)$$

where N_p is the number of nuclei in polycarions, and N is the total number of nuclei encountered in several microscopic fields. Usually, the number of nuclei (N) taken into account was 300–500. The background level of polynucleation in control preparations (without electric treatment), F_o, for all the cell lines was less than 5%.

Electron microscopy

Electron microscopy of the cell pellet was carried out according to conventional techniques. A modification of the setup allowed the introduction of a syringe needle through the chamber lid and the mounting of small stainless steel funnel, on the rotor head, connected to the needle by a Teflon tube. This made possible the introduction of the fixing solution (5% glutaraldehyde in PBS) directly into the chamber during centrifugation. Cells pelleted at 400 $\times g$ for 10 min, were (or were not in the control) subjected to high-voltage pulses. One minute following pulse delivery, 0.5 ml of glutaraldehyde solution was injected, while centrifugation continued for 10 more minutes. The pellet was fixed subsequently with 1% OsO_4 in 0.1 M phosphate buffer, dried and embedded in a mixture of Epon and Araldite (Merck). Ultra-thin sections were contrasted with the lead citrate and examined with a JEM 100 CX (Jeol) electron microscope.

Data reproducibility

All the qualitative regularities shown in the figures are well reproducible. However, the exact values of R_p and F may vary day-to-day, depending on the conditions of cell cultivation. Therefore, unless otherwise noted, each figure represents data of one typical experiment obtained on same cell sample, whereas the experiments of each type were reproduced at least 3 times.

Results

Effect of centrifugation on the cell pellet conductivity

The time-course of the conductivity of the chamber containing $1 \cdot 10^6$ L-cells upon stepwize increases of centripetal acceleration from 30 to 700 $\times g$ is shown in

Fig. 3. Within one minute of centrifugation at 34 $\times g$, cells sediment to the bottom and form a loose pellet, that corresponds to a decrease of 20–30% in chamber current. Further increases in G by spinning at 100–150 $\times g$ affect the chamber conductivity only slightly. At higher accelerations the chamber current relaxes quickly and then more slowly to a new level. After the centrifuge was stopped, the current relaxes partially within minutes.

The pellet resistance, R_p, depends on pellet porosity and geometry, the later is determined by the cross-sectional area and thickness of the pellet (i.e., number of cell layers, n). The $R_p(G)$-curves (compression curves) for L-cell pellets of different thickness are shown in Fig. 4a. A simple estimation shows that in the chamber with the 1-mm hole, one horizontal layer is formed by about $1.1 \cdot 10^4$ L cells of average diameter 12 μm. A thin pellet consisting of one or two cell layers does not show any noticeable rise in R_p in the range of accelerations used. When the number of cell layers in the pellet, n, is greater than 4, the R_p goes up markedly with the increase of G. The higher the n, the steeper the compression curve (Fig. 4a).

The form of the compression curves depends on the state of the cells. Cells preincubated at 4°C for 4 h become more rigid. The R_p for such pellets is lower for the same G than the resistance mesured for cells incubated at room temperature (data not shown). Irreversible damage of cells qualitatively changes the shape of compression curves. $R_p(G)$-curves for cells subjected to five pulses of 5 kV/cm, 100 μs each, and for cells killed by heating (60°C, 30 min), are shown in Fig. 4b. In contrast to normal cells, the resistance of such 'dead' pellets increases rapidly at low accelerations, but then reaches a plateau without further significant change.

A visco-elastic behavior of cells in pellets compressed by the centrifugal force presumably is determined by mechanical properties of the plasma membrane and of the cytoskeleton. While the cell is alive, there is no simple way to affect significantly the elasticity of the lipid membrane. However, the cytoskeleton can be easily weakened by depolymerizing its components such as actin microfilaments or microtubules [23]. The effects of cytochalasin B and colcemid on the resistance of pellets formed of L and 3T3 cells are shown in Fig. 5. Curves 1 and 5 correspond to compression of untreated L and 3T3 cells, respectively. After treatment with cytochalasin B (2 μg/ml) the slope of the compression curve for L-cells (curve 2) increased significantly, whereas the slope of the curve for 3T3 cells (curve 4) changed slightly. In order to obtain the same change in compressibility for 3T3 cells as for L cells, a 10-fold increase of cytochalasin B concentration was required. Compared with L cells, the 3T3 cells were greatly influenced by colcemid (0.5 μg/ml, curve 3). The compression curve for L cells in this case remained unchanged (not shown). It is noteworthy that cytochalasin B not only changed the slope of the compression curve for L cells, but also it prevented mechanical relaxation of cells after compression. After the centrifuge was stopped, the resistance of the cytochalasin B-treated pellet remained unchanged for more than 30 min (data not shown).

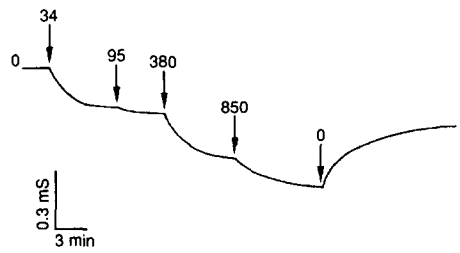

Fig. 3. The time-course of pellet conductivity upon compression by different centripetal accelerations (G). The chamber with a 3-mm hole contains $1 \cdot 10^6$ L cells. The accelerations denoted in g units were imposed at the moments shown by arrows.

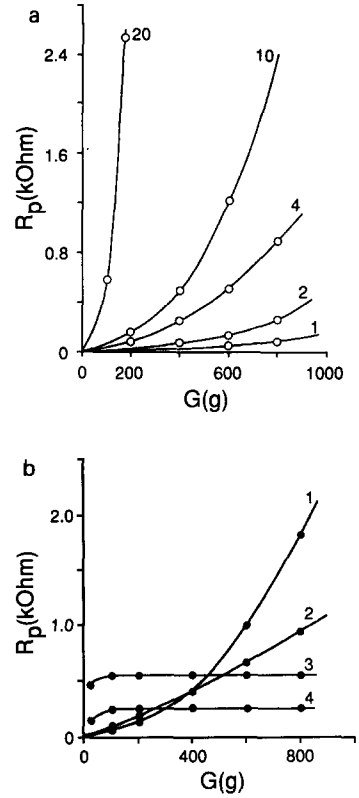

Fig. 4. Compression curves of L-cell pellets. (a) Cell pellet resistance (R_p) as a function of centripetal acceleration (G). Pellets of different thickness, from 1 to 20 cell layers (the numbers of layers are specified by the curves), were formed in a 1-mm hole chamber. (b) Compression curves for 10-layer pellets of intact L cells (curve 1) and cells pretreated with the high-voltage pulse (5 kV/cm, 100 μs) in the presence of 2 mM Ca^{2+}. Curves 4 and 3 correspond to 10- and 20-layer pellets, respectively, formed of cells subjected to 30-min heating to 60°C.

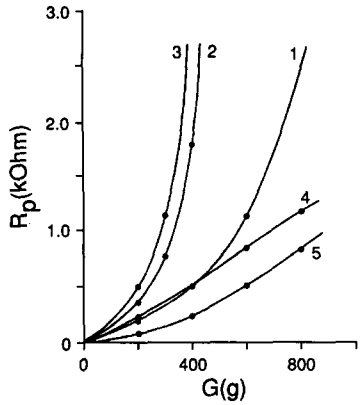

Fig. 5. Effects of cytochalasin B and colcemid on compression of L (curves 1 and 2) and 3T3 cells (curves 3–5) in pellets. Curves 1 and 5 correspond to untreated (control) cells. Curves 2 and 4 were obtained in the presence of 2 μg/ml cytochalasin B, curve 3 was measured in the presence of 0.5 μg/ml colcemid.

Electrical breakdown of cell membranes in the pellet

When the pellet of 10 or 20 cell layers was formed, the chamber resistance measured at low-voltage increased 3–5-fold. This confirmed that: (i), the membranes of intact cells retain their insulating properties and (ii), the pellet resistance becomes limiting in the circuit. Under these conditions, R_p is much higher than the series resistance of the buffer between the pellet and upper electrode, therefore almost all the voltage applied to the chamber electrodes drops across the pellet.

Application of high-voltage pulses led to a massive loss of the insulating properties of the membrane, i.e., to electric breakdown. The current of the L-cell pellet upon the square pulses of increasing amplitude is shown in Fig. 6. At low amplitude, the shape of current responses was close to rectangular and the values corresponded well enough to what was estimated from the pellet resistance, R_p, measured by the low-voltage AC test signal. When the pulse amplitude exceeded some threshold value (for a given duration), the shape of the current response changed. The current rose during the pulse, and its value at the end of the pulse showed non-linear dependence on the pulse amplitude.

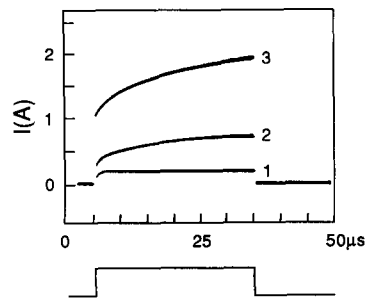

Fig. 6. Current oscillograms for pelleted cells at 30-μs square voltage pulses of different amplitudes: 20 (1), 60 (2) and 100 V (3). $2 \cdot 10^6$ L cells were pelleted in the 3 mm-hole chamber.

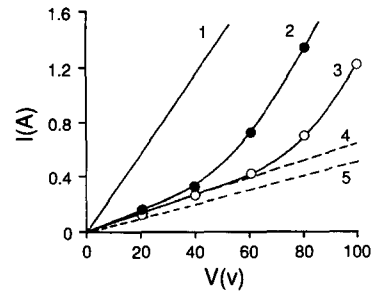

Fig. 7. 'Instant' current-to-voltage relationships taken for 10- and 20-layer L cell pellets (curves 2 and 3, respectively). Each dot represents chamber current measured at the end of a 30-μs pulse of a given amplitude. Curve 1 corresponds to the cell-free chamber filled with pulsation buffer only. Curves 4 and 5 were calculated on the basis of low-voltage AC measurements of pellet resistance.

The 'instant' current-to-voltage relationships taken for 10-and 20-layer pellets are shown in Fig. 7. Each dot represents current through the pellet measured at the end of 15-μs pulses for 10-and 20-layer pellets, (curves 2 and 3, respectively). The deflection point in the curves corresponds to the critical breakdown voltage. This value is higher for 20-layer pellets. It is noteworthy, that to the right of the deflection point, curves 2 and 3 are almost parallel to curve 1, which represents the current-to-voltage relationship for the chamber without cells (pulsation buffer only). The shift between curves 1 and 3, as well as between curves 1 and 2, is nearly equal to the critical breakdown voltage across the pellet in each case. A parallel layout of these curves shows that with the increase of pulse amplitude, the voltage across the pellet remains approximately constant and close to the critical one, while the pellet resistance decreases.

Membrane resealing after electric breakdown

When the amplitude and duration of the pulse are not extremely high, membrane breakdown is reversible, i.e., electropores reseal. The techniques employing entrapment of labeled molecules or ions [24] are limited in their time resolution, thus recording the membrane resealing process using electrical measurements on multicellular pellets may have several advantages. In the experiment, the cell pellets compressed by centrifugation (5 min, $400 \times g$) were subjected to a high-voltage pulse followed by a series of test pulses. The envelopes of current spikes upon the test pulses are shown in Fig. 8. Trace 1 is a base line recorded in response to test pulses, without breakdown pulse. The relaxation of cell pellet conductivity after application of 100, 200 and 300-V pulses (50-μs duration) is reflected by traces 2 through 4, respectively. The pellet conductivity decrease occurs in at least three stages. The first stage is fast (τ_1 approx. 0.5–1 ms), the second one is much slower (τ_2 approx. 10 s), while the complete relaxation of pellet conductivity to its initial value

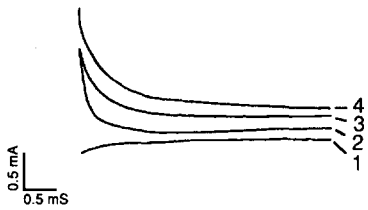

Fig. 8. Fast kinetics of cell membrane resealing after application of 50 μs-pulses with amplitudes: 0 (control), 100, 200 and 300 V (curves 1–4, respectively). The recording was carried out with the circuit shown in Fig. 2b. The pellet of L cells was subjected to single high-voltage pulses followed by a train of test pulses (10 V, 10-μs duration and 50-μs period). The envelopes of current spikes in response to test pulses are represented.

takes several minutes (the second and the third stages not shown).

Electrically-induced colloid-osmotic compression of cell pellets

After moderate electric treatment of the cell pellet in PBS, the pellet conductivity relaxes to a value remarkably lower than the initial one. The time-course of the current through the pellet of E2 cells in response to a low-voltage AC test signal after application of a 200-V, 30-μs pulse, is shown in Fig. 9 (curve 1). Bearing in mind a predictable loss of membrane insulating properties, as a result of electrical breakdown, one may expect an increase in pellet conductivity after pulse delivery. However, the observed effect is opposite. The measured current decreased gradually within tens of seconds for all the cell types examined. The osmotic nature of this effect was revealed in experiments carried out in the presence of osmoprotectants [7,8,25]: sucrose (100 mM) and bovine serum albumin (20 mg/ml). The pellet conductivity under these conditions changed only slightly upon pulse delivery (Fig. 9, curve 2).

The electron micrograph revealed dramatic changes in pellet porosity upon high-voltage treatment. Fig. 10a represents a thin section of a pellet of control E2 cells, which was fixed directly during the $400 \times g$ centrifugation. Cells bear many outgrowths and are separated, on average, by wide gaps of extracellular solution. After electric treatment with 200 V, 30-μs pulses, the cells are tightly packed: the extracellular space is almost eliminated and intermembrane contacts appear to be larger and closer (Fig. 10b). The extracellular liquid was presumably absorbed into the cells as a result of colloid-osmotic cell swelling after membrane permeabilization. At the same time, practically no changes in the cell packing were observed when the cells were pulse-treated in the presence of sucrose and bovine serum albumin, minimizing the colloid-osmotic swelling (same conditions as in Fig. 9, data not shown).

The extent of osmotic pellet compression is a non-monotonic function of the pulse amplitude. For instance, for the pellet containing $1 \cdot 10^6$ L cells, the increase of R_p begins at voltages close to the critical 'breakdown' voltage (Fig. 11, compare with Fig. 8), reaching a maximum at 125 V with a subsequent gradual decrease. Evidently, cells experienced stronger colloid-osmotic swelling when their membranes were permeabilized only to small inorganic ions [8]. Intensive electric treatment may induce larger pores providing exchange with many other compounds between the intra- and extra-cellular compartments, thus lowering or preventing cell swelling and consequently osmotic pellet compression.

Electrically-induced cell fusion in the centrifuge

Cells in pellets subjected to high-voltage pulses during intensive centrifugation fused forming numerous polycarions (Fig. 12). The fusion index, F, was dependent on pulse parameters, as well as on the centripetal acceleration, G. A dependence of F on pulse amplitude, measured for L cells at constant pulse duration (30 μs) and $G = 600 \times g$, is presented in Fig. 13. The voltage required for efficient fusion of these cells was several times the critical voltage inducing noticeable membrane poration (compare Fig. 7 and Fig. 13).

The index F of L-cell fusion induced by 30-μs pulses of three different amplitudes (400, 600 and 800 V) is plotted as a function of G in Fig. 14a. The low-voltage pellet resistance, R_p, measured before pulse delivery is shown by a dashed line (curve 4). The slight decrease in F observed at high accelerations and voltages (curves 2 and 3) may be attributed to cell damage by simultaneous action of these two factors. The increase in F was found to directly correlate with the rise of R_p. The treatment of L-cells with cytochalasin B led to an increase of F at low G, whereas at high accelerations, the fusion index was the same as in the control (Fig. 14b). In general, cytochalasin B affected fusion efficiency in the same way as it affected pellet resistance R_p (see Fig. 5).

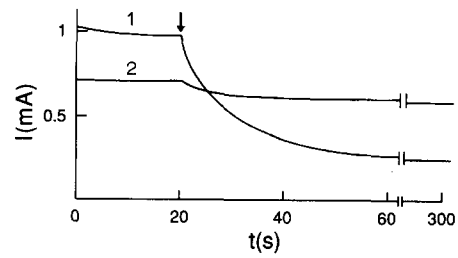

Fig. 9. The time-course of the current measured by 1 V, 10 kHz test signal on the pellet of $2 \cdot 10^6$ E2 cells before and after application of a 200-V, 30-μs pulse. Cells were pelleted in pure PBS (curve 1), and in PBS supplemented with 100 mM sucrose and 20 mg/ml of bovine serum albumin (curve 2). The moment of pulse application is shown by arrow.

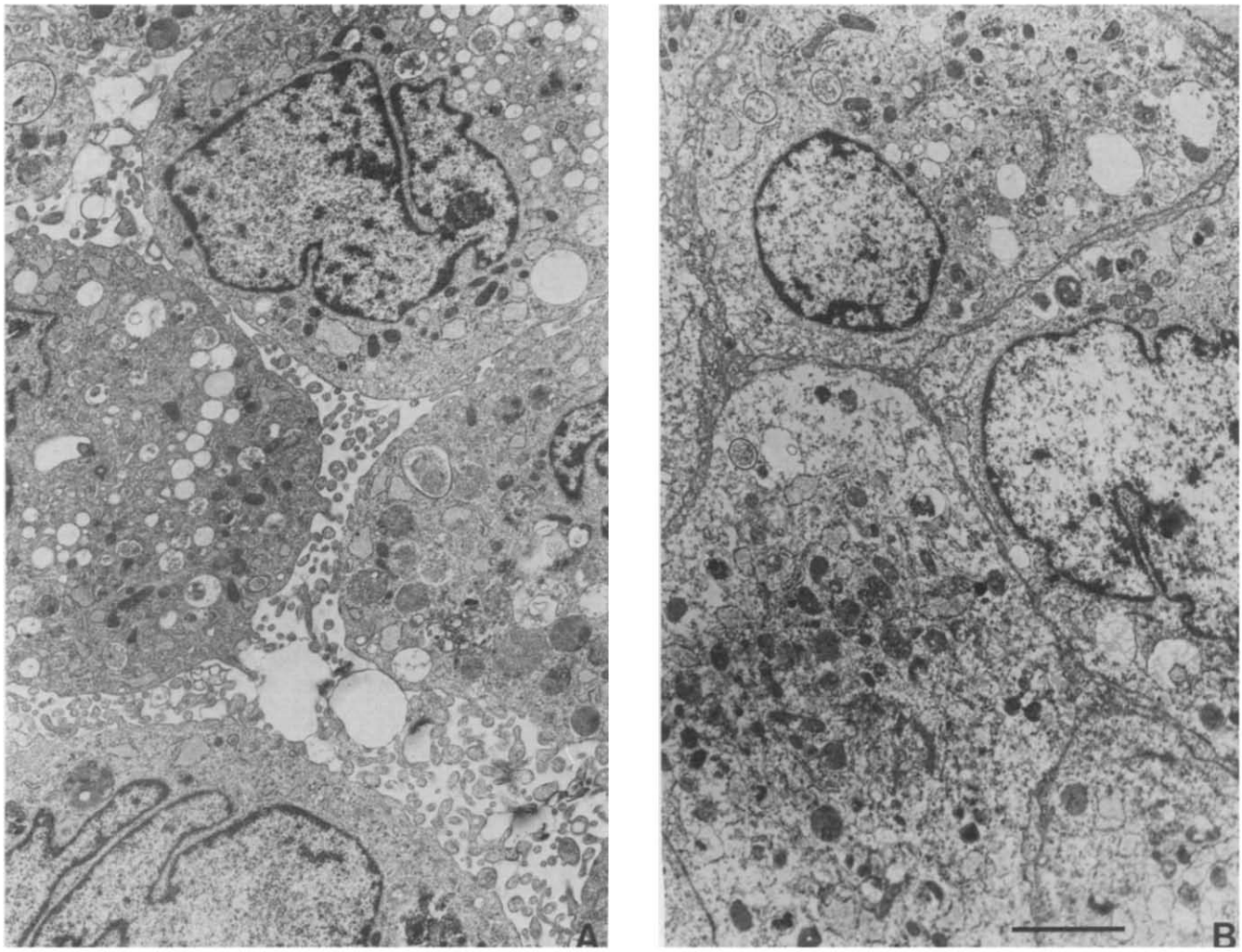

Fig. 10. Transmitting electron micrographs of E2 cells in pellets untreated (a), and treated (b) with a 200-V, 30-μs-pulse in PBS. The geometry of cell contacts in the pellet changed upon electric treatment. Bar = 2 μm.

In the next experiment tight L-cell pellets were formed by a $300 \times g$ centrifugation for 15 min, but the fusion pulse was applied a while after the centrifuge was stopped. The R_p was also controlled just prior to pulse application. The fusion index and R_p dependence on the time interval, t_d, between the centrifuge stoppage and fusion pulse delivery is shown in Fig. 15. Both values, R_p and F, decreased with t_d substantially and synchronously, that probably reflects the process of cell-shape relaxation and membrane gapping. The result suggests that the fusion efficiency is dramatically affected by reduction of membrane contact area.

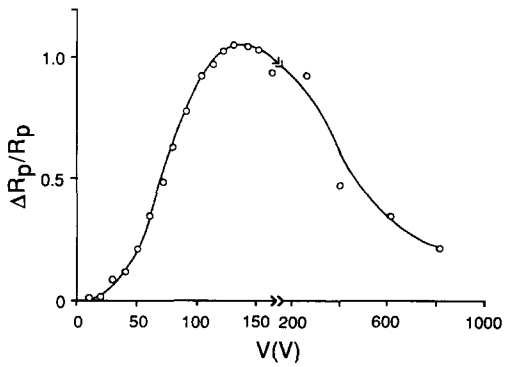

Fig. 11. The relative pellet resistance ($\Delta R_p/R_p$) as a function of high-voltage pulse amplitude. $1 \cdot 10^6$ L cells were pelleted in the 3-mm hole chamber. ΔR_p was measured 10 min following application of 30-μs pulses.

The additional factor which may increase the area and/or tightness of intermembrane contacts is the above-described colloid-osmotic pellet compression. This is illustrated by the following experiment. L cells were pelleted in PBS (with or without sucrose) at $400 \times g$ for 5 min. Immediately after rotor stoppage R_p was measured and the first pulse of 200 V for 30 μs was applied. A considerable increase in R_p was recorded within minutes. After a time interval ranging between 5 and 220 s, a second (fusion) pulse of 640 V

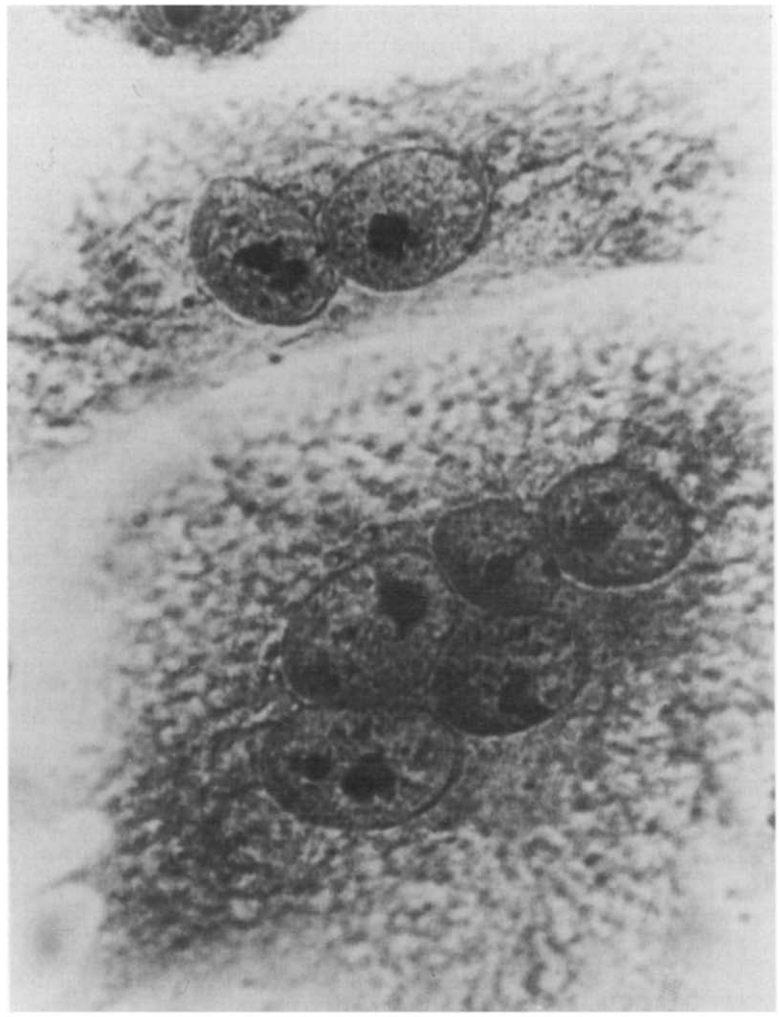

Fig. 12. Polycarions of CHO cells obtained by application of a single 400-V, 30-μs pulse on the cell pellet during centrifugation at 500 $\times$ g.

for 30 μs was applied. Fusion index was assayed as described in Materials and Methods. The data represented in Table I show that when the cells in the pellet are allowed to swell (R_p significantly increased), the F is relatively high. When the time interval between two pulses is short, or when the cells are placed in conditions suppressing colloid-osmotic swelling (sucrose in the medium), fusion yield is low.

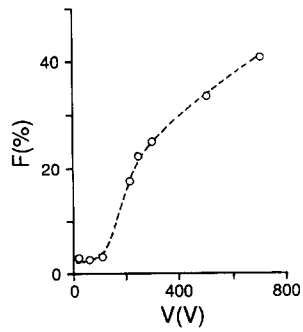

Fig. 13. The dependence of L-cell fusion index (F) on the pulse amplitude (V), taken at constant pulse duration 30 μs and centripetal acceleration $G = 600 \times g$.

To examine the possible existence of long-lived fusogenic state of the membranes after high-voltage pulse application [19,20], different cells (L-929, NIH3T3, HeLa, CHO and E2) were brought in tight contact either before or after the pulse treatment, and the resultant fusion yields were compared. Cells were pelleted at a very low acceleration (30 $\times$ g, 10 min) creating loose pellet. The pulse of 3–5 kV/cm, 30 μs was applied and immediately after this the acceleration was increased to 400–600 $\times$ g for 10 min, providing for fast pellet compression (pulse first protocol). In parallel, cells were first pelleted at 400 $\times$ g for 10 min, then one 30-μs pulse at 3 kV/cm, was applied, and centrifuga-

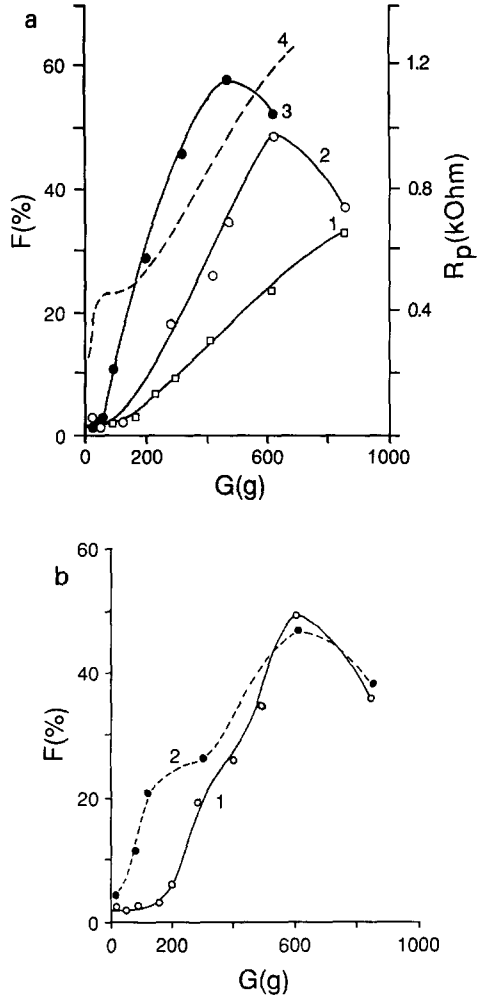

Fig. 14. Fusion index (F, solid lines) and the pellet resistance (R_p, dashed line) as functions of centripetal acceleration (G). (a) $1 \cdot 10^6$ L cells were pelleted for 5 min at given G. Then, after measuring R_p, single 30-μs pulses of 400 V (curve 1), 600 V (2) or 800 V (3) were applied at the same acceleration. Centrifugation continued for 3 more minutes and the fusion index (F) was determined. (b) The effect of cytochalasin B on the fusion index of L cells. Cytochalasin B-treated and untreated cells (control, curve 1) were pelleted for 10 min at a given acceleration and subjected to single pulses of 600 V, 30 μs, then F was determined as described in Materials and Methods.

tion continued at the same speed for 5 more minutes (contact first protocol). For all the cells examined, results were similar: F was in the range of 19–40% in the contact-first protocol, whereas in pulse-first protocol it was close to the level of spontaneous polynucleation for each type of cells and never exceeded 6% (data not shown). These data along with the data presented in Fig. 14a,b show that efficient cell electrofusion is possible only if cells are in close contact before the fusing pulse application.

The ionic strength of pulsation medium also may alter fusion [17,18,26]. A significant rise of F with the increase of NaCl concentration in the range of 0–100

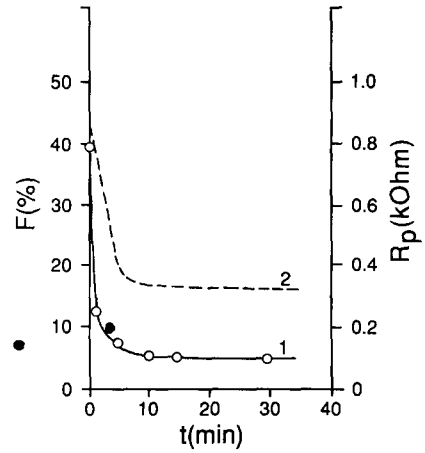

Fig. 15. Fusion index (F) and the pellet resistance (R_p) as functions of time interval between centrifuge stoppage and the moment of pulse application. $1 \cdot 10^6$ L cells were pelleted at $300 \times g$ for 15 min, then the centrifuge brake was turned on. In a given time interval after the rotor was stopped completely, R_p was measured and one pulse of 600 V, 30 μs was applied to the pellet. F was determined as described in Materials and Methods.

mM was observed on L cells fused in the centrifuge. However, for other cell types, F did not exhibit any distinct or monotonous dependence on ionic strength (data not shown).

Discussion

Cell pellets formed under controlled centrifugation conditions appear to be a convenient system for studying electrical, mechanical and osmotic properties of cells. As an important practical application, an effi-

TABLE I

The effect of colloid-osmotic pellet compression on fusion efficiency of L-929 cells

$1 \cdot 10^6$ L cells were pelleted by centrifugation ($400 \times g$, 5 min) in a 2-mm hole chamber. After complete stopping of the centrifuge two pulses of amplitudes U_1 and U_2 were applied with a time interval t_d between them. Pellet resistances, R_1 and R_2, were measured several seconds before the first and the second pulse respectively, using the low-voltage AC test signal. The fusion index, F, was determined as described in Materials and Methods. PBS was mixed with isotonic (290 mM) sucrose in 1:1 ratio to prevent cells from colloid-osmotic swelling.

Pulsation medium	R_1 (kΩ)	U_1 (V)	t_d (s)	R (kΩ)	U (V)	F (%)
PBS	2.55	690	220	10.8	0	4
	2.37	200	5	–	690	7.5
	2.40	200	120	7.75	690	20
	2.45	200	220	9.10	690	23
PBS + sucrose	4.96	690	220	4.98	0	4
	4.90	200	120	4.93	690	4.5
	4.95	200	220	4.95	690	4

cient cell electrofusion can be performed in a controllable manner using the centrifuge system. Two necessary conditions for cell electrofusion can be controlled independently: (i), tightness of intercellular contacts estimated by changes in pellet conductance and (ii), the extent of membrane poration monitored by measuring the breakdown current during the high-voltage pulse. To accomplish the optimal fusion conditions several parameters of the entire procedure can be adjusted. Besides electric parameters (amplitude, duration and number of pulses), the centripetal acceleration and the duration of centrifugation compressing cells before and after fusion pulse can be chosen in accordance to deformability and viability of a particular cell type. Cell electrofusion in the centrifuge can be readily performed in any biologically appropriate media, whereas other techniques, such as dielectrophoresis, restrict the choice of the medium composition [13]. The centrifuge electrofusion technique have been recently used for heterokaryon production in studies of DNA replication control [27].

The tightness of cells in the pellet appears to be directly correlated with pellet conductivity ($1/R_p$), which in turn is expected to be a linear function of pellet porosity. The pressure within the pellet is distributed non-uniformly: the cells near the bottom electrode are more compressed than cells in the top layers. A simple estimate shows that at acceleration $G = 1000 \times g$ and cell density $\rho = 1.07$ g/cm^3, the lower cells of 10-layer pellet experience a static pressure of about 100 Pa, which is sufficient to deform cells [28] and bring them in close contact. Cell deformation in the pellet during centrifugation is characterized qualitatively by the compression curves. These curves give an integral characteristic and cannot be related directly to the mechanical properties of individual cells. Nonetheless, our data for cytochalasin B- and colcemid-treated cells show that $R_p(G)$-dependences can be used to compare the averaged cell deformability in different conditions and emphasize the role of cytoskeleton in cell mechanics (Fig. 5). As seen from current kinetics in the course of pellet compression and subsequent relaxation (Fig. 3), cells experience the elastic (reversible) and the plastic (irreversible) deformation. Loss of ability to relax to the initial shape by cytochalasin B-treated L cells suggests that elastic properties of these cells are determined mainly by the F-actin component of the cytoskeleton. Studies of cell pellet relaxation may also give some insight to cell-to-cell agglutination and adhesion.

Compared with a cell suspension [10], the initial resistance of the cell pellet, R_p, is much higher. In fact, R_p is the limiting resistance in the circuit, therefore the main part of the voltage V applied to the electrodes drops across the pellet and the initial electric field intensity E in the pellet is higher than that predicted from the equation $E = V/d$, where d is the distance between the electrodes. For a pellet of 10 cell layers we detected electrical breakdown (poration) of membranes at a relatively low voltages ($V = 30$–40 V). In a tight pellet consisting of n cell layers, the voltage across each membrane can be estimated as $\Delta\phi = V/2n$. As the cell electroporation in the pellet of 20 cell layers begins at $V = 40$–60 V (Fig. 7), the critical transmembrane voltage can be estimated as 1–1.5 V. When V applied is much higher than the critical value, the pellet resistance drops almost instantly: the chamber current rises steeply within a fraction of μs and is not limited by R_p any longer. The voltage across the pellet drops to a lower value, which is close to the critical value (see Figs. 6 and 7) and is almost independent of the pulse amplitude. The system behaves as if it has a specific negative feedback, which preserves cells from irreversible damage in a wide range of pulse amplitudes.

The kinetics of the current increase at membrane breakdown (Fig. 6, traces 2 and 3) has two phases – fast and slow, and is similar to that recorded by Kinosita and Tsong on erythrocyte suspension [10]. The two phases presumably reflect fast pore formation and subsequent slow pore expansion. Similar regularities were observed on single cells using the patch-clamp technique [4] and also on planar bilayers [3,4]. It appears to be a common feature of cell and model lipid membranes.

The reverse process, i.e., membrane resealing, appears to proceed at least in three stages. A significant drop in pellet conductivity occured within a millisecond (Fig. 8) and was followed by two slower stages with characteristic times of about 10 s and 120 s, respectively. The fast stage may reflect rapid relaxation of pore radii upon field removal, as well as non-linear properties of numerous small pores [4]. Rapid relaxation of membrane conductivity after electrical breakdown has been also observed using voltage-sensitive dyes [29,30]. The slow stage is probably due to delayed resealing of wide hydrophilic and stabilized pores.

The cell electrofusion experiments presented may clarify some relationships between intermembrane contact formation, electroporation and resulting cell fusion. Tight intermembrane contacts established prior to fusing pulse delivery were found to be a prerequisite condition for cell fusion. We did not observe cell fusion for all cell lines in this study when the fusion pulse was applied before cell pelleting or without strong centrifugal pellet compression, even when a compressing force (600–$800 \times g$, 10 min) was applied within 20 s after pulse delivery. The fusion yield is higher if the fusing pulse is applied during intensive centrifugation, and drops dramatically when the pulse is applied after the centrifuge is stopped (Figs. 14 and 15). Electric pulse treatment under conditions of colloid-osmotic pellet

compression also increases fusion efficiency. These observations strongly suggest that cell electrofusion in the described system is not mediated by a long-lived fusogenic state [19,20], but is driven directly by the external electric field.

Cell electrofusion is highly correlated with electric pore formation and many authors regard the electropores as specific fusion sites [13,31–35]. Here we reported one more observation, which may implicate the direct effect of electric field on fusing membranes: the pulse amplitude which induces significant fusion is 3–4-times higher (200–300 V, 30 μs) than the critical amplitude leading to noticeable poration (80 V for a 20-layer pellet). It should be noted, that electrical detection of electropore formation in our experiments appears to be more sensitive than Trypan blue penetration tests used by others [36]. To explain the difference between the pulse amplitudes required for poration and fusion, we assume that besides pore formation, there is another stage in membrane electrofusion, which also depends on the electric field, but requires higher voltages.

The membrane electrofusion mechanism proposed by Kuzmin, Pastushenko and co-workers [34] predicts the following sequence of events. When the strong electric field is imposed on two cells in contact, the opposing membranes attract each other electrostatically [32–35,37,38]. At a supercritical field intensity pores are formed in both membranes: first in one, and then in the other. Asymmetrical pore formation in the first membrane should lead to a higher voltage drop across the second one, thus, formation of a nearly coaxial pore in the second membrane is to be preferential. The electric field configuration in the vicinity of coaxial pore pair creates strong attractive forces oriented normally to the plane of membranes and pressing the pore edges toward each other [34]. For the typical parameters ($\Delta\phi_m = 1$ V, membrane thickness 5 nm, and pore radius of 1 nm) the resulting pressure P_o focused in the edge of each pore was estimated as about 50 atm [34]. According to the theory, P_o is a square function of $\Delta\phi_m$, thus at sufficiently high voltages, the pressure is high enough to overcome electrostatic membrane repulsion, membrane resistivity to bending and, probably, hydration forces. Pore coupling by the action of electric field will result in merging of opposing membranes with the formation of intercellular cytoplasmic bridges followed by complete cell fusion.

The results presented above agree with the 'coaxial pore pair' model of membrane electrofusion [34], assuming that the electric field is a unique fusogenic factor, which not only destabilizes native membrane structure (poration), as many chemical fusogenes do [39,40], but provides strong attraction between contacting membranes [34,35], creates and matches numerous pores [34,35,41,42]. Recently this mechanism has been experimentally supported by the studies of erythrocyte ghost electrofusion kinetics [43].

Acknowledgements

The authors are grateful to V.Ph. Pastushenko, P.I. Kuzmin, Yu.A. Chizmadzhev and A.V. Zelenin for the interest in this work and fruitful discussion. Authors also thank L.I. Fedorova for maintaining cell cultures and W.J. Haynes for critical reading of the manuscript.

References

1 Coster, H.G.L. and Zimmermann, U. (1975) J. Membr. Biol. 22, 73–90.
2 Benz, R., Beckers, F. and Zimmermann, U. (1979) J. Membr. Biol. 48, 279–290.
3 Chernomordik, L.V., Sukharev, S.I., Abidor, I.G. and Chizmadzhev, Yu.A. (1983) Biochim. Biophys. Acta 736, 203–213.
4 Chernomordik, L.V., Sukharev, S.I., Popov, S.V., Pastushenko, V.F., Sokirko, A.V., Abidor I.G. and Chizmadzhev, Yu.A. (1987) Biochim. Biophys. Acta 902, 360–373.
5 Benz, R. and Zimmermann, U. (1980) Bioelectrochem. Bioenerg. 7, 723–739.
6 Benz, R. and Conti, F. (1981) Biochim. Biophys. Acta 645, 115–123.
7 Zimmermann, U., Pilwat, G., Holzapfel, C. and Rosenheck, K. (1976) J. Membr. Biol. 30, 135–152.
8 Kinosita, K., Jr. and Tsong, T.Y. (1977) Nature 268, 438–441.
9 Deuticke, B. and Schwister, K. (1989) in Electroporation and Electrofusion in Cell Biology (Neumann, E., Sowers, A.E., Jordan, C., eds.), pp. 127–148, Plenum Press, New York.
10 Kinosita, K., Jr. and Tsong, T.Y. (1979) Biochim. Biophys. Acta 554, 479–497.
11 Teissie, J. and Tsong, T.Y. (1980) J. Membr. Biol. 55, 133–140.
12 Senda, M., Takeda, J., Abe, S. and Nakamura, T. (1979) Plant Cell Physiol. 20, 1491–1493.
13 Zimmermann, U. (1986) Rev. Physiol. Biochem. Pharmacol. 105, 175–255.
14 Karsten, U., Stolley, P. and Seidel, B. (1992) in Guide to Electroporation and Electrofusion (Chang, D.C., Chassey, B.M., Saunders, J.A., Sowers, A.E., eds.), pp. 363–369, Academic Press, San Diego.
15 Henery, C.C. and Kaufman, M.H. (1992) Mol. Reprod. Dev. 32, 251–258.
16 Weber, H., Forster, W., Jacob, H.-E. and Berg, H. (1981) Z. Allg. Microbiol. 21, 555–562.
17 Finaz, C., Lefevre, A. and Teissie, J. (1984) Exp. Cell. Res. 150, 477–482.
18 Sukharev, S.I., Bandrina, I.N., Barbul, A.I., Fedorova, L.I. Abidor, I.G. and Zelenin, A.V. (1990) Biochim. Biophys. Acta 1034, 125–131.
19 Teissie, J. and Rols, M.P. (1986) Biochem. Biophys. Res. Commun. 140, 258–261.
20 Sowers, A.E. (1986) J. Cell Biol. 102, 1358–1362.
21 Abidor, I.G., Barbul, A.I., Zhelev, D., Sukharev, S.I., Bandrina, I.N., Fedorova, L.I., Pastushenko, V.Ph., Kuzmin, P.I. and Zelenin, A.V. (1989) Biol. Membrany 6, 1296–1312. (Russian)
22 Sukharev, S.I. (1989) Bielectrochem. Bioenerg. 21, 179–191.
23 Vasiliev, J.M. (1985) Biochim. Biophys. Acta. 737, 305–341.
24 Serperzu, E.H., Kinosita, K., Jr. and Tsong, T.Y. (1985) Biochim. Biophys. Acta 812, 779–785.

25 Herzog, R., Mueller-Wellensiek, A. and Vaelther, W. (1987) Life Sci. 39, 2279–2288.
26 Blangero, C. and Teissie, J. (1985) J. Membr. Biol. 86, 247–253.
27 Prudovsky, I.A., Kosimov, R.B., Sukharev, S.I., Pospelova, T.V., Prasolov, V.S. and Zelenin, A.V. (1993) Cell Prolif. 26, 221–233
28 Evans, E.A. and Skalak, R. (1980) Mechanics and Thermodynamics of Biomembranes, CRC Press, Boca Raton.
29 Kinosita, K., Ashikawa, I., Saita, N., Yoshimura, H., Itoh, H., Nagayama, K. and Ikegami, A. (1988) Biophys. J. 53, 1015–1019.
30 Hibino, M., Itoh, H. and Kinosita, K. (1993) Biophys. J. 64, 1789–1800.
31 Zimmermann, U. (1982) Biochim. Biophys. Acta 694, 227–277.
32 Zhelev, D., Dimitrov, D. and Doinov, P. (1988) Bioelectrochem. Bioenerg. 20, 155–167.
33 Sugar, I.P., Forster, W. and Neumann, E. (1987) Biophys. Chem. 26, 321–331.
34 Kuzmin, P.I., Pastushenko, V.Ph., Abidor, I.G., Sukharev, S.I., Barbul, A.I. and Chizmadzhev, Yu.A. (1988) Biol. Membrany. 5, 600–612. (Russian)
35 Stenger, D.A., and Hui, S.-W. (1986) J. Membr. Biol. 93, 43–53.
36 Teissie, J. and Rols, M.-P. (1993) Biophys. J. 65, 409–413.
37 Stenger, D.A., Kaler, K.V.I.S. and Hui, S.W. (1991) Biophys. J. 59, 1074–1084.
38 Dimitrov, D.S. and Zhelev, D.V. (1988) Progr. Colloid Polym. Sci. 76, 109–112.
39 Ringertz, N.R. and Savage, R.E. (1976) Cell Hybrids, Academic Press, New York.
40 Roos, D.S. (1981) in Membrane Fusion (Wilschut, J. and Hoekstra, D., eds.), pp. 649–663, Marcel Dekker, New York.
41 Dimitrov, D. and Jain, R. (1984) Biochim. Biophys. Acta 779, 437–468.
42 Dimitrov, D., Zhelev, D. and Jain, R. (1985) J. Theor. Biol. 113, 353–377.
43 Abidor, I.G. and Sowers, A. (1992) Biophys. J. 61, 1557–1569.